Hyperspectral subpixel target detection based on extended mathematical morphology

Liu Chang, Li Junwei

(Science and Technology on Optical Radiation Laboratory, Beijing 100854, China)

Abstract: A hyperspectral subpixel target detection algorithm was proposed based on extended mathematical morphology and spectral angle mapping. The spectral and spatial information had been used to locate and detect targets under the condition that prior knowledge of targets and background was unknown. Then hyperspectral subpixel targets was detected and recognized. The extended mathematical morphological erosion and dilation operations were performed respectively to extract endmembers. The spectral angle mapping method was used to detect and recognize interested targets. The hyperspectral image collected by AVIRIS was applied to evaluate the proposed algorithm. The proposed algorithm was compared with SAM algorithm and RX algorithm by a specifically designed experiment. From the results of the experiments, it is illuminated that the proposed algorithm can detect subpixel targets with low false alarm rate and its performance is better than that of the other algorithms under the same condition.

Key words: extended mathematical morphology; spectral angle mapping; hyperspectral image endmember extraction; subpixel target detection

CLC number: TP751 **Document code:** A **Article ID:** 1007-2276(2015)10-3141-07

基于扩展数学形态学的高光谱亚像元目标检测

刘 畅,李军伟

(光学辐射重点实验室,北京 100854)

摘 要: 提出了一种基于扩展数学形态学和光谱角度匹配相结合的高光谱亚像元目标检测算法。在目标与背景未知的情况下,同时利用光谱和空间信息实现目标的定位与检测,实现高光谱亚像元目标的检测识别。通过扩展的形态学膨胀和腐蚀运算实现端元提取,采用光谱角度匹配算法进行感兴趣目标的检测识别。算法性能通过 AVIRIS 数据进行评价,与仅利用光谱角度匹配的算法和 RX 异常检测算法进行比较。实验证明,所提出的算法性能优于其他两种算法,具有低虚警率的亚像元目标检测结果。

关键词: 扩展数学形态学; 光谱角度匹配; 高光谱图像; 端元提取; 亚像元目标检测

收稿日期:2015-02-20; **修订日期**:2015-03-28

作者简介:刘畅(1988-),男,工程师,硕士,研究方向为高光谱目标特性技术和光谱数据处理技术等。Email:531093626@qq.com

0 Introduction

The rising of hyperspectral remote sensing is one of the greatest achievements in 1980 s. Hyperspectral target detection technology is the most important application direction of hyperspectral remote sensing. Popularly based on that assumed data obeys some statistical or geometrical model, traditional target detection algorithms structure detection operator and estimate the statistical parameters of the operator according to the prior information, such as Adaptive Cosine/Coherence Estimator (ACE), Orthogonal Subspace Projector(OSP) algorithm[1] etc. But in the practical application, the prior information of targets is not easy to get.

Under the condition that the target and background are unknown, the target detection can complicate using two methods. One is anomaly target detection directly according to the distribution of the information, such as Reed −x Detection (RXD) algorithm, Uniform Target Detection (UTD) algorithm etc. The other is unsupervised subpixel detection using endmember extraction algorithms in unmixing technology to get the target and background information. Usually, because of the limit of spatial resolution in remote images and the complexity of land objects, some interested targets mostly exist in the image in the form of mixed pixels. So, it is very important to study the subpixel target detection and recognition technology based on endmember extraction algorithm[1].

Traditional subpixel target detection algorithms based on endmember extraction algorithm only consider data′s spectral information and ignore the spatial correlation between pixels. For the more accurate analysis of hyperspectral remote images, it is very necessary to consider the spectral and spatial information comprehensively. So, we proposed a subpixel target detection algorithm using the extended mathematical morphology algorithm and the Spectral Angle Mapping (SAM) algorithm. This algorithm uses extended morphology erosion and dilation operations to extract endmembers. It effectively combines spectral and spatial information. Then use the spectral angle mapping algorithm to extract interested targets. This algorithm overcomes the disadvantage that the SAM algorithm is sensitive to spectral signature and when unmixed pixels widely exist, classification accuracy will be very low. And it effectively inhibits the effects of background and noise and reduces false alarm rate. To validate the algorithm performance, we conducted experiments using real remote sensing data and analyzed the results.

1 Hyperspectral subpixel target detection based on extended mathematical morphology

1.1 Basic operations of mathematical morphology

Dilation and erosion is the two basic operations of mathematical morphology. They were first defined for binary image and extended to grayscale image afterward. The dilation and erosion operation for the image $f(x,y)$ using K is shown as follows:

$$d(x,y)=(f\oplus K)(x,y)=\mathrm{Sup}(f(x,y),K)=\mathrm{Max}_{(s,t)\in K}\{f(x+s,y+t)+k(s,t)\} \quad (1)$$

$$e(x,y)=(f\otimes K)(x,y)=\mathrm{In}f(f(x,y),K)=\mathrm{Min}_{(s,t)\in K}\{f(x+s,y+t)-k(s,t)\} \quad (2)$$

where $k(s,t)$ means corresponding weight of different elements in structure elements.

1.2 Extended mathematical morphology operation in hyperspectral image

In grayscale morphology, we can calculate maximum or minimum gray value directly based on the numerical size of pixels as ordering relation. But in hyperspectral image, this operation is not feasible. Because any pixel in hyperspectral image is multidimensional and we cannot use a direct method to simply compare the size of different pixels. So the biggest problem extending mathematical morphology operation to hyperspectral image is how to sort the

pixels in the multi-dimensional space according to a specific comparison relationship[2].

Because every pixel in hyperspectral image is multi-dimensional, the basis of selecting pixels is the purity of pixels. According to convex geometry theory, the hyperspectral data corresponds to a convex simplex in the feature space. Pure pixels usually exists on the edge of the convex simplex, and the most spectrally mixed pixels exist in the center of the convex simplex. So we can infer their positions in the convex simplex by comparing the space distance between pixels. And then we can get the purity information.

In 2002, Plaza proposed a endmember extraction algorithm[3]. This algorithm has realized the automated endmember extraction of the hyperspectral images using extended mathematical morphology operation. This algorithm has extended the definition of traditional mathematical morphology theory and combined the spatial information and the spectral information of the hyperspectral image effectively. In history, he first applied the traditional morphological operations(dilation and erosion) based on binary image to hyperspectral image. In China, Guo Rui et al. also studied this algorithm[4]. On the basis of this, the algorithm is further studied in this paper and the performance of the algorithm is improved.

We use Spectral Angle Distance (SAD) in this paper to calculate the distance between multi-dimensional vectors. Assume a group of multi-dimensional vectors of one pixel′s spatial neighborhood is $V(x_i,y_j,w)$ $i=1,2,\cdots,b,w=1,2,\cdots,n$ (x and y represent the spatial coordinates of the point, $a\times b$ is the size of the spatial neighborhood, n is the band dimension). Then the SAD of any two vectors $V(x_{i1}, y_{j1},w)$, $V(x_{i2},y_{j2},w)$ can represent in radian as follows:

$$\mathrm{dist}(V(x_{i1},y_{j1},w),\ V(x_{i2},y_{j2},w))= \arccos\left(\frac{V(x_{i1},y_{j1},w)\cdot V(x_{i2},y_{j2},w)}{\|V(x_{i1},y_{j1},w)\|\cdot\|V(x_{i2},y_{j2},w)\|}\right) \quad (3)$$

At the basis of this distance definition, we can expand the definition of the dilation and erosion operation. In order to determine the ordering relation of the multi-dimensional vectors, Plaza introduced a metric operator of the multi-dimensional vector into hyperspectral image processing. This metric operator calculate the cumulative distance from one pixel to other pixels in the structure element. If the size of the structure element is too big, the computational algorithm will be quite large and the computational complexity has reached $o(n^4)$. In order to improve the algorithm efficiency, we calculate the distance between one pixel to the centroid instead. The computation has been significantly reduced and the computational complexity is only $o(n^2)$.

In the structure element K, the centroid defines as follows:

$$c_K=\frac{1}{M}\sum_s\sum_t f(s,t,w),\ \forall(s,t,w)\in K,\ w=1,2,\cdots,n \quad (4)$$

where M represents the number of pixels in the structure element. The distance of one pixel $f(x,y,w)$, $w=1,2,\cdots,n$ in the structure element K to the centroid defines as follows:

$$D(f(x,y,w),\ K)=\mathrm{dist}(f(x,y,w),c_K) \quad (5)$$

Then, the dilation and erosion operation can be expressed as follows:

$$d(x,y,w)=(f\oplus K)(x,y,w)= \mathrm{arg\_Max}_{(s,t,w)\in K}\{D(f(x+s,y+t,w),K)\} \quad (6)$$

$$e(x,y,w)=(f\ominus K)(x,y,w)= \mathrm{arg\_Min}_{(s,t,w)\in K}\{D(f(x-s,y-t,w),K)\} \quad (7)$$

where arg_Max and arg_Min represent the pixel vectors that make the distance D to the centroid max and min and correspond to the most spectrally singular and the most spectrally mixed pixels within a kernel K, as shown in Fig.1.

Then, use Morphological Eccentricity Index (MEI) to express the pixel purity in the structure element[5]. MEI is the SAD between the most spectrally singular and the most spectrally mixed pixels. It defines as follows:

$$\mathrm{MEI}(x,y,w)=\mathrm{dist}(d(x,y,w),e(x,y,w)),\ w=1,2,\cdots,n \quad (8)$$

MEI image characterizes the purity information

of the original hyperspectral image. The greater gray value the pixel has, the corresponding pixel in the original image is more likely to be endmember.

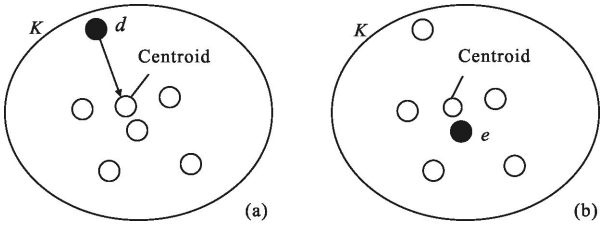

Fig.1 Calculation of the most spectrally singular (a) and the most spectrally mixed (b) pixels within a kernel K by using the distance to the centroid D

1.3 Hyperspectral subpixel target detection based on extended mathematical morphology

For the target detection in hyperspectral image, although the extended dilation operation effectively uses spectral and spatial information, it also artificially adds noise or background and limits the false alarm rate of the algorithm. So in order to effectively suppress background effect, and quantifying the difference between target and background, and overcoming the disadvantage that when unmixed pixels widely exist, the classification accuracy of the SAM algorithm will be very low, we proposed a subpixel target detection algorithm using the extended mathematical morphology algorithm and the spectral angle mapping algorithm. The specific implementation steps are as follows (as shown in Fig.2):

(1) Read the original hyperspectral image, use the minimum structure element K_{min}, carry out dilation and erosion operation based on centroid in structure element to each pixel in target hyperspectral image. Find the purest pixel d (x,y,w) and the most mixed pixel $e(x,y,w)$, and calculate the corresponding MEI;

(2) Increase the size of the structure element, repeat step (1) until the maximum structure element K_{max}. Calculate MEI value repeatedly and record them. Take the average value of the corresponding pixels at the same coordinate point. Then we can get the final MEI image;

(3) Carry out threshold judgment, get the average of all the pixels′ gray value in the MEI image as the set threshold. The pixel in the MEI image whose value is bigger than the threshold will be labeled as pure pixel (endmember);

(4) Carry out image segmentation and region growing[6] in the final endmember image to complete automatic selection of endmembers;

(5) Using the endmember spectra we get, carry out the SAM algorithm to complete the detection and recognition of the interested targets.

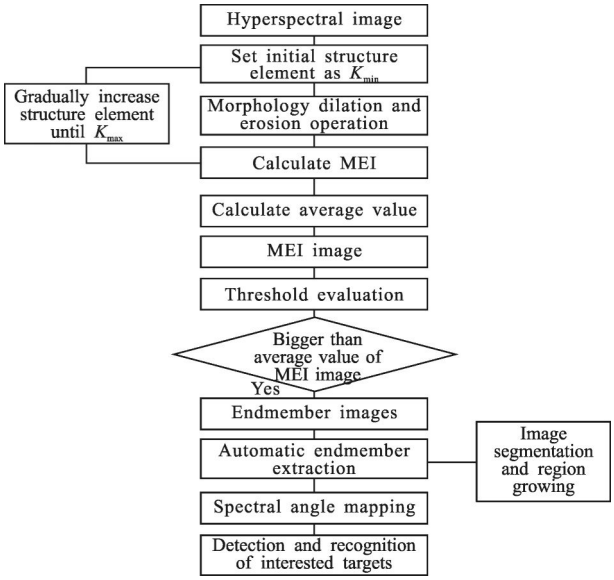

Fig.2 Flow chart of the hyperspectral subpixel target detection algorithm based on extended mathematical morphology

2 Experiment and analysis

2.1 Experiment data

The hyperspectral image used in this article is the Navy airfield data which is acquired in San Diego, California, United States by the AVIRIS sensor. This image has applied ENVI FLAASH module to conduct atmospheric correction and generated a reflectance image. This data set contains 224 bands and the wavelength range is from 0.37 μm to 2.51 μm. As shown in Fig.3, it is AVIRIS data′s false color composite image which is used for processing (Band 28,19,10).

Fig.3 Navy airfield AVIRIS data′s false color composite image in San Diego, California, United States(Band 28,19,10)

2.2 Experiment analysis

There are some kinds of planes in the image that we use. The ones at(232,136) and (244,144) are the most striking, and at around (89,11), there are also some other planes. First, use the extended mathematical morphology algorithm to extract endmembers of the image, and we can get the endmember spectra of the planes at the three coordinates as shown in Fig.4.

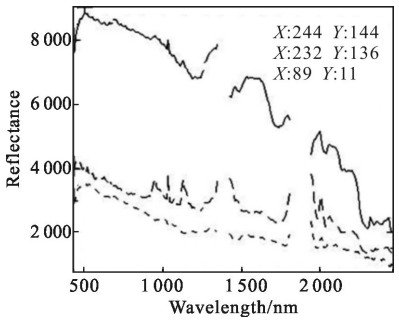

Fig.4 Image of three planes′ spectra extracted by extended mathematical morphology endmember extraction algorithm

Then, for the three planes′ spectra extracted, use the spectral angle mapping algorithm to detect and recognize the plane targets. The spectra are seen as multidimensional vectors in the spectral angle mapping algorithm and calculate the generalized angle between the two spectrum (pixel spectrum and reference spectrum) vectors. The smaller the angle, the more similar the spectra. And classify the unknown spectra according to a given similarity threshold[3]. The detection result is shown in Fig.5.

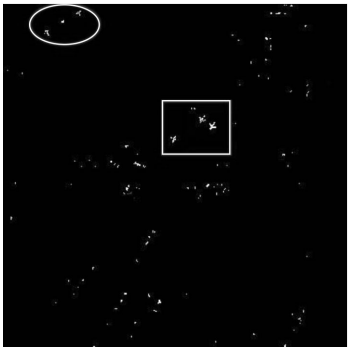

Fig.5 Plane targets′ detection result image using the proposed algorithm

To validate the algorithm performance, use the spectral angle mapping algorithm, the RX anomaly detection algorithm, the ACE algorithm and the adaptive matched filter (AMF) algorithm to detect and recognize the plane targets as comparison and analysis. The RX anomaly detection algorithm is developed by the Reed and Yu[7]. The form of the RX detection operator is

$$\delta_{\mathrm{RXD}}(r)=(r-u)^{\mathrm{T}}K^{-1}(r-u) \tag{9}$$

where r is anyone of the pixel vectors in the image; μ is the sample mean vector; K is the sample covariance matrix of the image.

See the details of the ACE algorithm and the AMF algorithm in references [8−10].

The detection result images of the plane targets using the two algorithms are shown in Fig.6. Compare Fig.5 and Fig.6 and we can conclude that the algorithm we proposed can detect and recognize subpixel targets effectively. And the algorithm has low false alarm rate 0.024 6% and high detection rate 97.32%; The false alarm rate using SAM algorithm (as shown in Fig.6 (a)) is 0.0428% and the detection rate is 94.6%; the false alarm rate using RX algorithm (as shown in Fig.6 (b)) is 0.1236% and the detection rate is 89.6%; the false alarm rate using ACE algorithm (as shown in Fig.6 (c)) is 0.061 4% and the detection rate is 92.2%; the false alarm rate using AMF algorithm (as shown in Fig.6(d)) is 0.052 8% and the detection rate is 93.1%. The detection results (as shown in Tab.1) prove that compared with the

SAM algorithm, the RX algorithm, the ACE algorithm and the AMF algorithm, the performance of the subpixel target detection and recognition algorithm we proposed using spectral and spatial information has improved significantly.

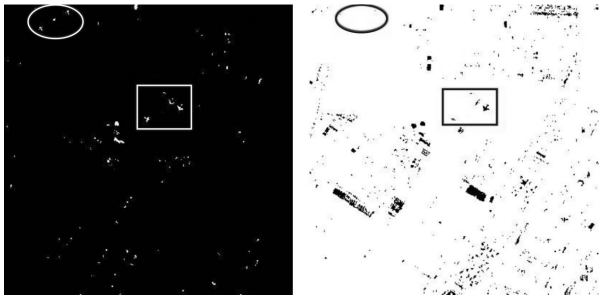

(a) Using SAM algorithm (b) Using RX algorithm

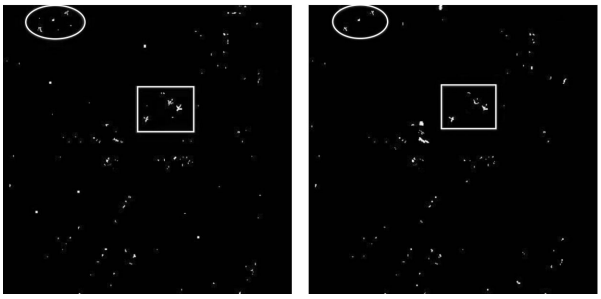

(c) Using ACE algorithm (d) Using AMF algorithm

Fig.6 Plane targets′ detection result images using the other four algorithms

Tab.1 Results of different algorithms

Algorithm	False alarm rate	Detection rate
This paper′s	0.024 6%	97.32%
SAM	0.042 8%	94.6%
RX	0.123 6%	89.6%
ACE	0.061 4%	92.2%
AMF	0.052 8%	93.1%

3 Conclusion

Hyperspectral target detection technology is the most important application direction of hyperspectral remote sensing. Traditional subpixel target detection algorithms based on endmember extraction algorithm only consider data′s spectral information and ignore the spatial correlation between pixels. Based on this, we proposed a subpixel target detection algorithm using the extended mathematical morphology algorithm and the spectral angle mapping algorithm. This algorithm uses extended morphology erosion and dilation operations to extract endmembers. It effectively combines spectral and spatial information. Then use the spectral angle mapping algorithm to extract interested targets. This algorithm overcomes the disadvantage that the SAM algorithm is sensitive to spectral signature and when unmixed pixels widely exist, classification accuracy will be very low. And it effectively inhibits the effects of background and noise and reduces false alarm rate.

To validate the algorithm performance, apply the proposed algorithm to a real hyperspectral image and use SAM, RX, ACE and AMF algorithm as comparison and analysis. The results show that the algorithm we proposed can detect and recognize hyperspectral subpixel targets effectively. Compared with the other algorithms, this algorithm has low false alarm rate and high detection rate. The false alarm rate of our algorithm is 0.024 6% and the detection rate is 97.32%; the false alarm rate using SAM algorithm is 0.042 8% and the detection rate is 94.6%; the false alarm rate using RX algorithm is 0.123 6% and the detection rate is 89.6%; the false alarm rate using ACE algorithm is 0.061 4% and the detection rate is 92.2%; the false alarm rate using AMF algorithm is 0.052 8% and the detection rate is 93.1%. It proved that the algorithm we proposed reduced the false alarm rate and increased the detection rate of subpixel targets.

References:

[1] Manolakis D, Shaw G. Detection algorithms for hyperspectral imaging applications [J]. ***IEEE Signal Processing Magazine***, 2002, 19(1): 29-43.

[2] Zhang Xiongfei. The design and application of the hyperspectral database based on the web [D]. Beijing:

Institute of Remote Sensing and Digital Earth, Chinese Academy of Sciences, 2003. (in Chinese)

[3] Plaza A, Martinez P, Perez R, et al. A new method for target detection in hyperspectral imagery based on extended morphological profiles [C]//Geoscience and Remote Sensing Symposium IEEE, 2003, 6: 3772-3774.

[4] Guo Rui, Li Na, Zhao Huijie, et al. Anomaly detection based on extended mathematical morphology for hyperspectral imagery [J]. ***Acta Optica Sinica***, 2008, 28(8): 1480-1484.

[5] Antonio Plaza, Pablo Martinez, Rosa Perez, et al. A quantitative and comparative analysis of endmember extraction algorithms from hyperspectral data [J]. ***IEEE Transactions on Geoscienee and Remote Sensing***, 2004, 42 (3): 651-654.

[6] Liu Li, Jiao Binliang, Liu Qinlong. The promotion and realization of Otsu multi-threshold segmentation method [J]. ***Science of Surveying and Mapping***, 2009, 34 (6): 240-241. (in Chinese)

[7] Reed I S, Yu X. Adaptive multiple-band CFAR detection of an optical pattern with unknown spectral distribution [J]. ***IEEE Transactions on Acoustic Speech and Signal Process***, 2000, 38(10): 1760-1770.

[8] Manolakis D, Lockwood R, Codey T, et al. Is there a best hyperspectral detection algorithm? [C]//SPIE Newsroom, 2009: 1-3.

[9] Pieper M L, Manolakis D, Lockwood R, et al. Hyperspectral detection and discrimination using the ACE algorithm [C]// SPIE, 2011, 8158: 815807.

[10] Jiang Chaoshu, Li Hongbin, Rangaswamy M. Conjugate gradient parametric adaptive matched filter [C]//Radar Conference, IEEE, 2010: 1097-5659.